Applied Radiation and Isotopes, to be published

Observation of Radiation Effects on Three-Dimensional Optical Random-Access-Memory Materials for Use in Radiation Dosimetry

Abbreviated Title: **Radiation Effects on 3D ORAM Material**

Gary W. Phillips[1,2], Amy K. Readshaw[2], Gerald O. Brown[3], Richard G. Weiss[3], Noel A. Guardala[4], Jack L. Price[4], Susette C. Mueller[2], and Marko Moscovitch[2]

1. U.S. Naval Research Laboratory, 4555 Overlook Avenue SW, Washington, DC 20375
2. Georgetown University Medical Center, 3970 Reservoir Road NW, Washington, DC 20007
3. Georgetown University, Department of Chemistry, 37th & O Street NW, Washington, DC 20057
4. Naval Surface Warfare Center, Carderock Division, 9500 MacArthur Boulevard, West Bethesda, MD 20817

address correspondence to:
Gary W. Phillips
Code 6616
Naval Research Laboratory
Washington, DC 20375

phone (202) 767-5466, fax (202) 404-8076
e-mail: gary.phillips@nrl.navy.mil

Abstract

The first experimental investigation has been performed of radiation effects on three-dimensional optical random-access-memory materials. Thin films of poly(methyl methacrylate) doped with spirobenzopyran were irradiated with uniform fluxes of protons, alpha particles and $^{12}C^{+3}$ ions at fixed energies per nucleon from 0.5 to 2.5 MeV and fluences from 10^{10} to 10^{14} cm^{-2}. The exposed films were examined under a confocal laser scanning microscopy system which is capable of optically sectioning the materials. The irradiation resulted in a permanent change in the materials from a non-fluorescent form to a form which is fluorescent under both 488 nm and 514 nm excitation. Profiles were measured of fluorescent intensity versus depth and of intensity versus dose. It was found that both the particle energy and the dose can be obtained from measuring the width of the depth profile and the fluorescent intensity. These properties are very promising for dosimetry applications since they allow calculation of an accurate dose equivalent.

Introduction

Three-dimensional optical random access memories (3D ORAMs) make use of photosensitive materials for large volume storage of computer data. Typical 3D ORAM materials are comprised of photochromic molecules such as spirobenzopyran (SP) which can exist as two distinct geometrical isomers embedded in a polymer matrix (Ford, 1993, Dvornikov *et al*., 1994). Information is stored at the intersection of two laser beams by a two-photon excitation process that converts the material from its more stable isomer (representing a binary zero bit) to a less stable isomer (representing a binary one.) In the case of SP, the less stable isomer exhibits stimulated fluorescence upon absorption of a photon and decay back to the more stable state.

The use of 3D ORAM materials to record energy transferred by energetic neutrons or heavy charged particles (HCPs) was originally proposed by one of the present authors (Moscovitch, 1994, 1996). Recent theoretical calculations indicate that passage of ionizing radiation through 3D ORAM materials should alter the information in a way that is dependent on the energy transferred to the material, allowing a record of the exposure to be read out (Moscovitch, 1997). The model predicts that the magnitude and radial extent of the effect is dependent on both dose and linear energy transfer (LET).

A variety of approaches have been used or proposed for neutron dosimetry. All depend on charged particle interactions to detect the neutrons and all suffer from severe energy dependence or other limitations (Griffith, 1988). The neutron personnel dosimetry systems most commonly used today are based on the effect of albedo-thermoluminescence (Devine, 1990). Thermoluminescent dosimeters (TLDs) are primarily sensitive to thermal neutrons. In order to provide sensitivity to energetic neutrons these systems make use of the albedo effect whereby neutrons are moderated to thermal energies through scattering in the body of the wearer. This method suffers from severe energy dependence, which may result in an error of as much as a factor of 10-100 if the neutron energy spectrum is not precisely known.

3D ORAMs show promise of being able to correlate the neutron energy spectrum with secondary particle track characteristics such as energy distribution, shape and size in order to calculate a more accurate dose equivalent. In addition, because of their sensitivity to HCPs, dosimeters based on 3D ORAM materials could provide detailed information on particle type and energy distribution for HCPs allowing more accurate dosimetry for persons in earth orbit or in space. This paper reports on the first experiments to determine the effects of exposure of 3D ORAM materials to ionizing radiation. Uniform beams of protons, alpha particles and $^{12}C^{+3}$ ions from a particle accelerator were used for this initial study because their energy and fluence could be precisely controlled and measured.

Materials and Methods

The 3D ORAM material used for this experiment consisted of the photochromic molecule spirobenzopyran (SP) embedded in a matrix of poly(methyl methacrylate) (PMMA) at SP concentrations of 1% and 0.1% (by weight). The SP (6'-nitro-1,3,3-trimethylindolino-benzospiropyran) was synthesized by an adaptation of the method used by Audic and Gautron (Audic, 1968).

A mixture of 1.30 g (7.78 mmol) of 2-hydroxyl-5-nitrobenzaldehyde and 1.35 g (7.79 mmol) of 2-methylene-1,3,3-trimethyl indoline in dry methanol was refluxed under a nitrogen atmosphere for

5 h in the dark. The crude dark purple product was filtered and dried in the dark for 24 h. The amount obtained was 2.20 g (88% yield). After recrystallization from benzene, the yield obtained was 0.72 g (29% yield). The melting point range of these light orange crystals was 173.0-176.1 ^{0}C compared to the literature value of 176 ^{0}C (Audic, 1968).

A quantity of 7.27 g of purified PMMA (Ohta, 1996) was dissolved in 40 ml of chloroform. The solution was stirred and refluxed at a constant temperature of 90 ^{o}C for 2 h. Then 73 mg (0.23 mmol) of SP was added. The solution immediately became dark blue. It was stirred for 30 min. and cast on glass plates covered with aluminum foil. After being dried under vacuum in the dark for 5 days, the transparent films were peeled from the foil. The thickness of the films ranged from 50-70 μm and the concentration of SP was 3.8 x 10^{-2} M (1% by weight) according to optical density measurements using a Perkin-Elmer Lambda 6 UV/Vis absorption spectrophotometer.

The films were exposed to beams of protons at energies of 0.6 to 2.5 MeV, alpha particles at 2 and 5 MeV, and $^{12}C^{+3}$ ions at 6.5 MeV from the 3MV NEC Pelletron tandem accelerator operated by the Naval Surface Warfare Center, Carderock Division, at White Oak, MD (Price, 1991). This facility has two negative ion sources at 30^o on either side of the accelerator axis, an Alphatross rf source for gaseous elements and a SNICS cesium sputter source for solids. Negative ions from the source in use are injected by a magnet into the low-energy end of the tandem accelerator and are accelerated toward the positive terminal at the center of the accelerator. At the terminal the ions are stripped of two or more electrons using a nitrogen stripper gas. The now-positive ions are accelerated away from the terminal and exit at the high-energy end of the tandem accelerator. Mass-energy analysis of the high-energy beam is accomplished by a 90^o analyzing magnet. A switching magnet is then used to steer the beam to one of several experimental beam lines. Beam dynamics and control are accomplished by the use of several magnetic and electrostatic focusing and steering elements. A feedback signal from slits at the exit of the analyzing magnet is used to control the terminal voltage and stabilize the beam energy.

The less stable isomer of the SP molecule in PMMA has a half-life for thermal de-excitation of about 30 minutes at room temperature, too short for convenient exposure to radiation and measurement of the effects. Instead, for the initial experiments exposures were made with the SP in its more stable isomeric form. Exposures were made at fluences from 10^{10} to 10^{14} cm^{-2} using uniform beams over a 3 mm diameter aperture at fluxes varying from 2 x 10^9 to 4.5 x 10^{10} s^{-1}cm^{-2}. These fluxes were at the low end of the capability of the accelerator and were obtained by defocusing the beam and/or sweeping the beam over the target aperture.

These exposures resulted in local doses in the films which varied from 10^3 to 10^7 Gy. The dose *D* in Gray is calculated by

$$D = (1.6 \times 10^{-10}) FE/R\rho$$

where *F* is the fluence in particles per cm^2, *E* is the particle energy in MeV, *R* is the calculated particle range in cm, and ρ is the density of the stopping material in g/cm^3 (ρ = 1.2 g/cm^3 for PMMA.) The ranges of the ion beams in PMMA were calculated using the SRIM/TRIM code (Ziegler, 1988). These varied from 7.3 μm for 6.5 MeV ^{12}C to 88 μm for 2.5 MeV protons. This expression gives an average of the dose deposited along the track. Charged particles tend to deposit a larger amount of energy toward the end of the track (the Bragg "peak"), however in most cases we did not have the resolution to observe this.

The exposed spots were examined under a BIORAD MRC-600 Confocal Laser Scanning Microscope System (CLSM), located at the Georgetown University Medical Center, Washington, DC. With the CLSM it is possible to section the material optically in order to look at effects of the exposure versus depth. This device uses an argon ion laser beam with selectable beams of 488 nm and 514 nm which are focused to a spot at a selected depth in the sample. Deflection mirrors are used to scan the spot in the focal plane in order to create a two-dimensional image. Fluorescence from the sample is viewed through the same optics as the incident laser beam and then through a barrier filter which blocks reflected laser light but passes wavelengths >515 nm for 488 nm excitation and >550 nm for 514 nm excitation. An aperture at the image plane restricts the image to the focal spot in the sample. The spot intensities are recorded with a photomultiplier and converted into a 2D image which is displayed on a video monitor. After each 2D scan, a stepping motor is used to shift the focal plane in depth. This produces a series of 2D images versus depth which are stored in computer memory and can be played back to form a 3D image. Effective resolution was about 1 μm in the scanning plane by a few μm in depth. This resolution was insufficient to observe individual particle tracks but was sufficient to detect changes in the material on the scale of a few μm.

Fluorescent intensities were determined from the computer images by taking the average image intensity at each depth over a rectangle at a fixed size of 100 x 67 pixels. The range of intensities greatly exceeded the 0 to 255 dynamic range of the video image. To account for this, the image intensity was adjusted by one or more of the following methods: 1) by insertion of a neutral density filter in front of the laser output, 2) by adjusting the image aperture, or 3) by adjusting the photomultiplier gain. When a change was made in the filter, aperture or gain, the same sample was analyzed before and after the change to provide a relative normalization factor for the intensities.

Results and Discussion

These initial studies were done with relatively high dose levels in order to quantitatively determine the effect of HCP radiation on 3D ORAM material. No effort was made to use low dose levels which are typical to radiation protection applications. The limitation to high dose levels was determined by the capabilities of the particle accelerator.

Exposure of the SP doped PMMA films to HCP radiation resulted in a permanent change in the SP molecule. The unexposed films were clear, but exposure resulted in a visible yellow beam spot at the higher fluences, as can be seen in the photograph of Figure 1. The exposed spots were found to fluoresce when examined using the CLSM under excitation at either 488 or 514 nm. The 488 nm wavelength excitation was used for the results reported here because it resulted in 20-30% higher intensity fluorescence than for the 514 nm excitation. Fluorescence was observed for all exposures, even the lower fluences which did not produce a visible beam spot on the films. Furthermore, the fluorescent intensity was undiminished after a period of several weeks. This is distinctly different from the behavior of the less stable form of the SP molecule (which is fluorescent only at excitation wavelengths above 500 nm and is thermally unstable at room temperature.) To rule out changes in the PMMA, films without the SP molecule were also exposed at some of the higher fluences. No visible change was observed in these films and no fluorescence was observed under the CLSM.

For the SP doped PMMA films, profiles of fluorescent intensity versus depth were measured using the CLSM. Figure 2 shows the depth profiles for 0.6 MeV to 2.5 MeV protons normalized to a maximum intensity of 200 (arbitrary units). These are plotted versus the relative depth obtained

from the CLSM focal depth. The surface of the film is on the left side of the curves and the position of the left half-maximum is arbitrarily taken as zero depth since there is no clear indication of the surface position in the CLSM images. There appears to be evidence of a Bragg peak in the 2 MeV profile which peaks at about 30 relative depth. This is not apparent in the 2.5 MeV profile since the proton range at this energy exceeds the film thickness. Rather there is a slight attenuation of the intensity with depth in the film over the range of 20-50 in relative depth. Similar depth profile measurements were obtained for 2 and 5 MeV alpha particles and 6.5 MeV ^{12}C.

The full-width at half-maximum (FWHM) of the depth profiles is plotted against energy per nucleon in figure 3. The curve is a quadratic fit to the data. ***This is a significant result for dosimetry applications since it shows that the energy of the incident particles can be determined by measuring the FWHM of the depth profiles.*** Within the limited range in energy/nucleon measured here, the 0.5 and 1.25 MeV/amu alpha particles and the 0.625 MeV/amu ^{12}C ions appear to lie on the same curve as the protons.

To see how the intensities varied for the different particles and energies measured in this study, the fluorescent intensities from the CLSM analysis were compared at the depth of maximum intensity in each film. Figure 4 shows a plot of the maximum fluorescent intensities for films exposed to 0.6, 1.0 and 2.5 MeV protons, 6.5 MeV ^{12}C ions, and 2.0 and 5.0 MeV alpha particles plotted versus the dose. The top three plots in figure 4 are for films of PMMA doped with SP at the 1% level, while the bottom three plots are for films doped at the 0.1% level. The lines in the figure are smooth curves fitted to the data points.

The intensity for a given particle and energy increases monotonically with dose over a range of several orders of magnitude before saturating at the higher doses, with the exception of the 5 MeV alpha particle intensity at 3.9 x 10^4 Gy which is less than the intensity at 1.9 x 10^4 Gy. The latter point seams to be anomalously high and causes an apparent oscillation in the curve fitted to the data. There is no obvious explanation for this behavior, but it could be due to non-uniformities in the particle beam or in the film.

The data for an SP concentration of 1% are approximately a factor of 10 higher than the data for an SP concentration of 0.1%, showing that the effect depends on the SP concentration. This figure also shows that for a given particle, dose and SP concentration, particles with higher energy have an increased fluorescent effect on the films. Note that the saturation level at high doses for a given particle and SP concentration also occurs at higher intensities for higher particle energies.

Table 1 compares the maximum fluorescent intensities at 100 kGy. At a given SP concentration and particle type, the intensity varies with particle energy and inversely with LET. The intensity for 2.5 MeV protons is significantly greater than for 0.6 MeV protons and similarly the intensity for 5 MeV alphas is significantly greater than for 2 MeV alphas.

Theoretical calculations of HCP track structure in solids (Kiefer, 1986) indicate that the penumbra radius or maximum radial extent r_{max} of the track depends only on the maximum energy transfer ϵ_{max} from the ion to a secondary electron in the solid, which is proportional to the energy per nucleon *E/A*. The maximum energy transfer to an electron of mass m_e is given by

$$\epsilon_{max} = 2m_e c^2 \beta^2$$

for non-relativistic particles ($\beta \ll 1$), where β is the particle velocity *v* divided by *c* the speed of light. For an ion of mass *M*, this expression becomes

$$\epsilon_{max} = 4\,(m_e/M)\,E \cong .002\,E/\mathrm{A}.$$

For PMMA with a density of 1.2 g/cm^2, the empirical expression for the maximum radius is given by

$$r_{max} = 44\,(E/A)^{\alpha}\ \mathrm{nm}$$

where the fitting parameter $\alpha = 1.7$ and E is given in MeV. Thus the maximum track radius depends only on $(E/A)^{\alpha}$. However, the radial dose follows a $1/r^2$ dependence, so most of the energy is deposited at much smaller radii. Theoretical calculations for HCP tracks in SP doped PMMA indicate that the probability of conversion of the SP from the fluorescent form to the non-fluorescent form saturates at a probability of 1 for small radii less than some radius r_o which increases with effective charge and thus with LET (Moscovitch, 1997). For particles with energy of 1 MeV/amu this saturation extends out to a value of r_o = 2 nm for protons, 4 nm for alphas, and 10 nm for ^{12}C nuclei. At radii less than r_o the energy density exceeds that necessary to totally convert the SP and the excess energy is wasted. We appear to be seeing a similar phenomenon here since the higher LET particles are less effective at producing changes in the SP doped PMMA films.

This effect is similar to that which is observed in organic scintillators where it has been attributed to quenching of the primary excitation by the high density of ionized and excited molecules (Birks, 1964). The quenching occurs primarily for high LET particles (alpha particles with energy < 6 MeV and protons < 2 MeV) which is about the range of the energies in the current study. As a result, there is a linear relationship between the fluorescent intensity *L* and the residual range *r* of the particle. If this explanation is correct, we should expect to see the effect become negligible for higher energy particles where the energy density in the track decreases below that necessary for saturation..

Conclusions

We have investigated for the first time the effects of ionizing radiation on 3D ORAM materials. These results support the possible use of these materials as radiation detectors/dosimeters. We observe a permanent change in the fluorescent properties of SP doped PMMA exposed to protons, alpha particles and $^{12}C^{+3}$ ions in the range of 0.5 to 2.5 MeV/amu. Fluorescence was observed using a confocal laser scanning microscope and the depth profiles were measured as a function of particle energy per nucleon. In the range of energies investigated, the fluorescent intensity at a fixed dose varies with particle type and energy. These studies were performed at relatively high dose and future efforts will be directed at investigating the effects at lower doses. *However, the properties of these materials observed in the current study are very promising for dosimetry use since the energy and dose can both be determined from a combination of penetration depth and fluorescent intensity, thus allowing calculation of an accurate dose equivalent.*

Acknowledgments

This work was supported by NASA, Life and Biomedical Sciences Applications Division (Grant No. 9307-0347), by the U.S. Department of Energy Health Physics Faculty Research Award program administered by Oak Ridge Associated Universities under Management and Operating Contract No.

DE-AC05-76OR00003, by the National Science Foundation (RGW and GOB) and by an Interdisciplinary Grant from Georgetown University President Rev. Leo O'Donovan. One of us (GWP) was supported by the Naval Research Laboratory Advanced Graduate Research Program while on sabbatical at the Georgetown University Medical Center. We would like to thank Janice Hicks of the Georgetown University Chemistry Department for valuable preliminary discussions on this project.

References

Audic, C. and Gautron, R. (1968) Photochromisme des Indolino-Spiropyrannes. *Bull. Soc. Chim.*, 2075-2077.

Birks J. B. (1964) The Theory and Practice of Scintillation Counting. Pergamon Press, Oxford, New York.

Ford J. E., Hunter S., Piyaket R., Esener S. E., Dvornikov A. S. and Rentzepis P. M. (1993) 3-D Two Photon Memory Materials and Systems. *Organic and Biological Optoelectronics, SPIE* **1853**, 5-13.

Devine R. T., Moscovitch M. and Blake P. K. (1990) The US Naval Dosimetry Center Thermoluminescence Dosimetry System. *Radiation Protection Dosimetry* **30**, 231-236.

Dvornikov A. S., Esener S. E. and Rentzepis P. M. (1994) Three-Dimensional Optical Storage Memory by Means of Two-Photon Interaction. *Optical Computing Hardware*, Jahns J. and Lee S. H. (Eds), Academic Press Inc., Boston, 287-325.

Griffith R. V. (1988) Review of the State of the Art in Personnel Neutron Monitoring with Solid State Detectors. *Radiation Protection Dosimetry* **23,** 155-160.

Kiefer J. and Straaten H. (1986) A Model of Ion Track Structure Based on Classical Collision Dynamics. *Phys. Med. Biol.* **31**, 1201-1209.

Knoll G. F. (1989) *Radiation Detection and Measurement*, 2nd Ed., John Wiley & Sons, New York.

Moscovitch M. (1994) Neutron Dosimetry Using Three-Dimensional Optical Memory. U.S. Patent 5,319,210.

Moscovitch M. (1996) Neutron Spectrometer, Real-Time Dosimeter and Methodology Using Three-Dimensional Optical Memory. U.S. Patent 5,498,876.

Moscovitch M. and Emfietzoglou D. (1997) Simulation of Radiation Effects on Three-Dimensional Computer Optical Memories. *J. Appl. Phys*. **81**, 58-69.

Ohta N., Koizumi M., Umeuchi S., Nishimura Y. and Yamazaki I. (1996) External Electric Field Effects on Fluorescence in an Electron Donor and Acceptor System: Ethyl Carbazole and Dimethyl Terephthalate in PMMA Polymer Films. *J. Phys. Chem.* **100**, 16466-16471.

Price J. L., Land D. J., Stern S. H., Guardala N. A., Cady P. K., Simons D. G., Brown M. D., Brennan J. G. and Stumborg M. F. (1991) An Overview of the Ion-Beam Analysis Laboratory at White Oak. *Nucl. Instr. and Meth. in Phys. Res.* **B56**, 1014-1016.

Ziegler J. F. and Manoyan, J. M. (1988) The Stopping Power of Ions in Compounds. *Nucl. Instr. and Meth. in Phys. Res.* **B35**, 215-228.

Table 1. Comparison of LET to fluorescent intensities at 100 kGy for irradiation of PMMA by heavy charged particles

particle (%SP)	energy (MeV)	energy/nucleon (MeV/amu)	range* (μm)	initial LET* (keV/μm)	average LET† (keV/μm)	fluorescent intensity#
protons (1%)	2.50	2.50	88.4	17	28	140
protons (1%)	0.60	0.60	8.9	46	67	57
^{12}C (1%)	6.50	0.54	7.3	1009	890	21
protons (0.1%)	1.00	1.00	19.4	33	52	8.5
alphas (0.1%)	5.00	1.25	29.6	112	169	6.5
alphas (0.1%)	2.00	0.50	8.6	199	233	1.5

*calculated using SRIM/TRIM (Ziegler, 1988), †energy/range, #relative units

Figure Captions

1. This photograph shows the visible beam spots as a results of exposure of films of SP doped PMMA to 2.5 MeV proton beams. The SP concentration was 1% except in the far right film which was pure PMMA. From left to right the exposures were 4, 37, 171, 796, and 374 kGy.
2. CLSM Depth profiles for protons on SP doped PMMA. Similar depth profiles are seen for 2 and 5 MeV alpha particles and 6.5 MeV ^{12}C ions. The lines are smooth curves drawn through the data.
3. Full width at half maximum (FWHM) for CLSM depth profiles versus energy per nucleon. The line is a second order polynomial fit to the data.
4. Maximum fluorescent intensities from the CLSM analysis plotted versus dose for the indicated particle and energy. The lines are smooth curves drawn through the data.

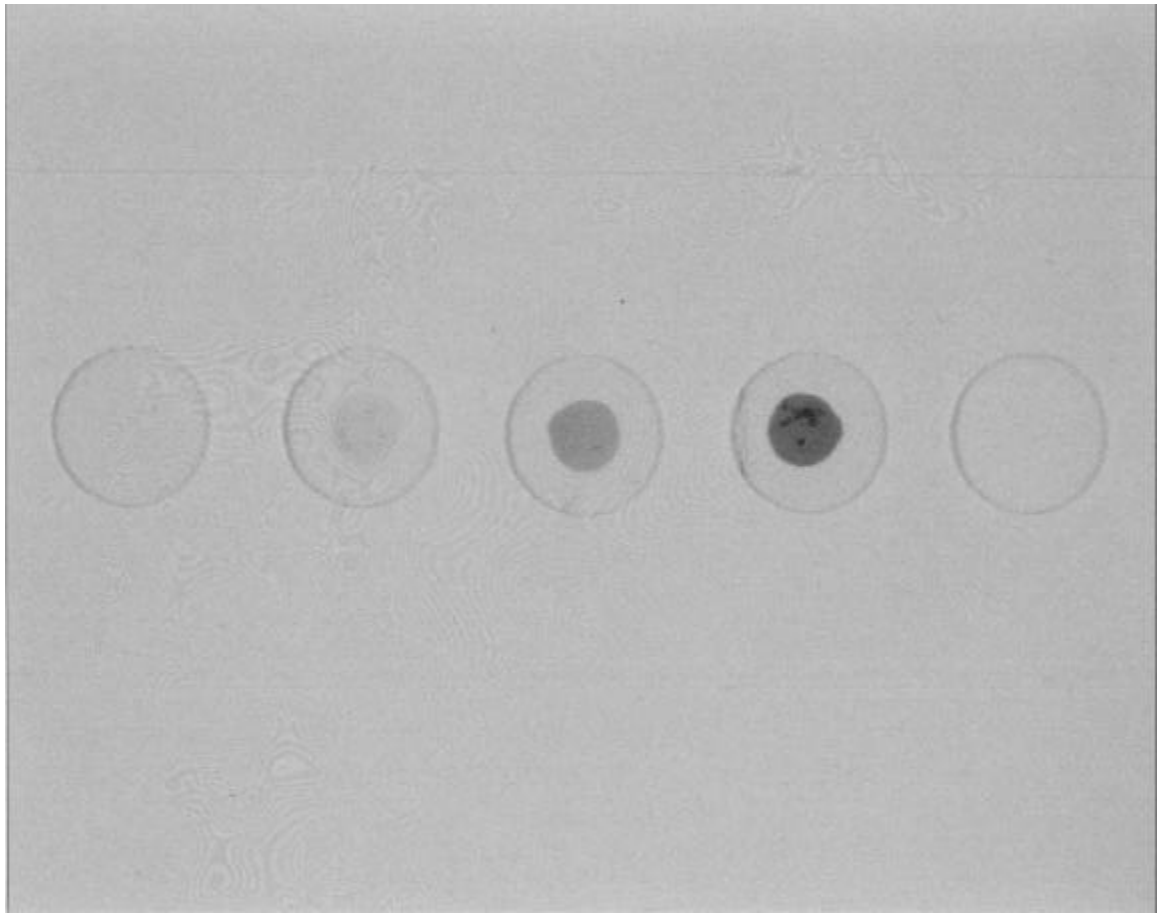

Figure 1. This photograph shows the visible beam spots as a results of exposure of films of SP doped PMMA to 2.5 MeV proton beams. The SP concentration was 1% except in the far right film which was pure PMMA. From left to right the exposures were 4, 37, 171, 796, and 374 kGy.

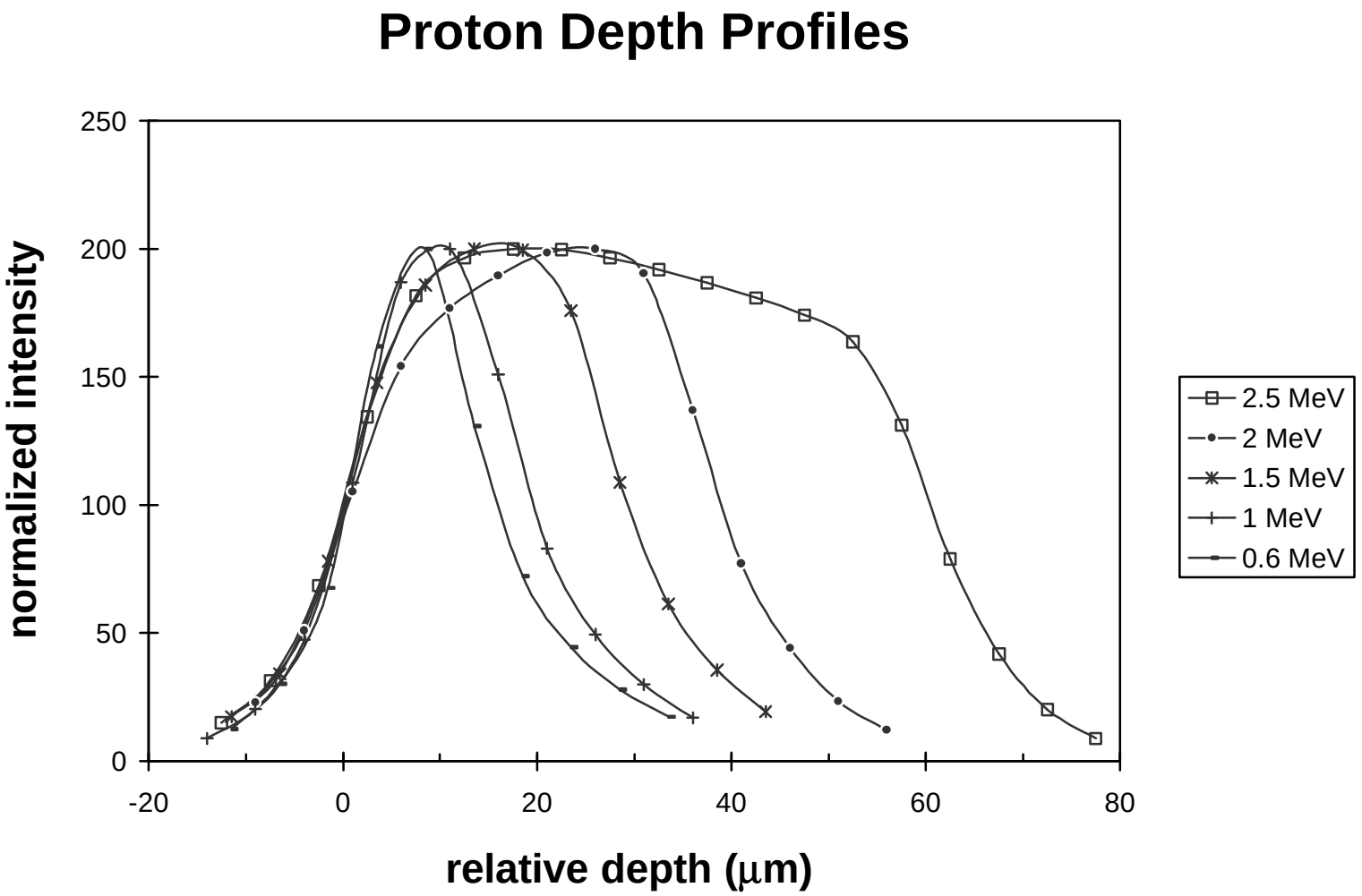

Figure 2. CLSM Depth profiles for protons on SP doped PMMA. Similar depth profiles are seen for 2 and 5 MeV alpha particles and 6.5 MeV 12C ions. The lines are smooth curves drawn through the data.

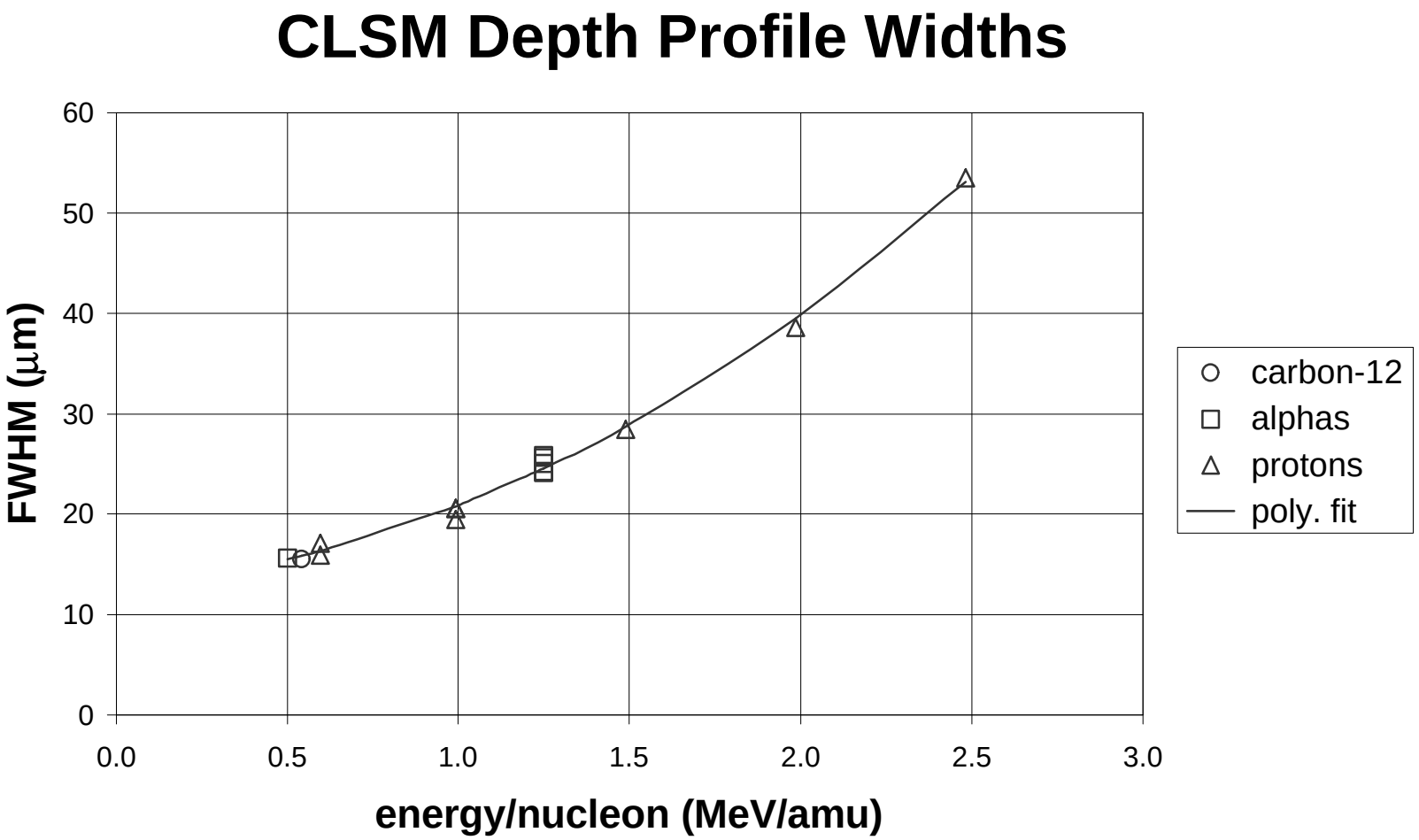

Figure 3. Full width at half maximum (FWHM) for CLSM depth profiles versus energy per nucleon. The line is a second order polynomial fit to the data.

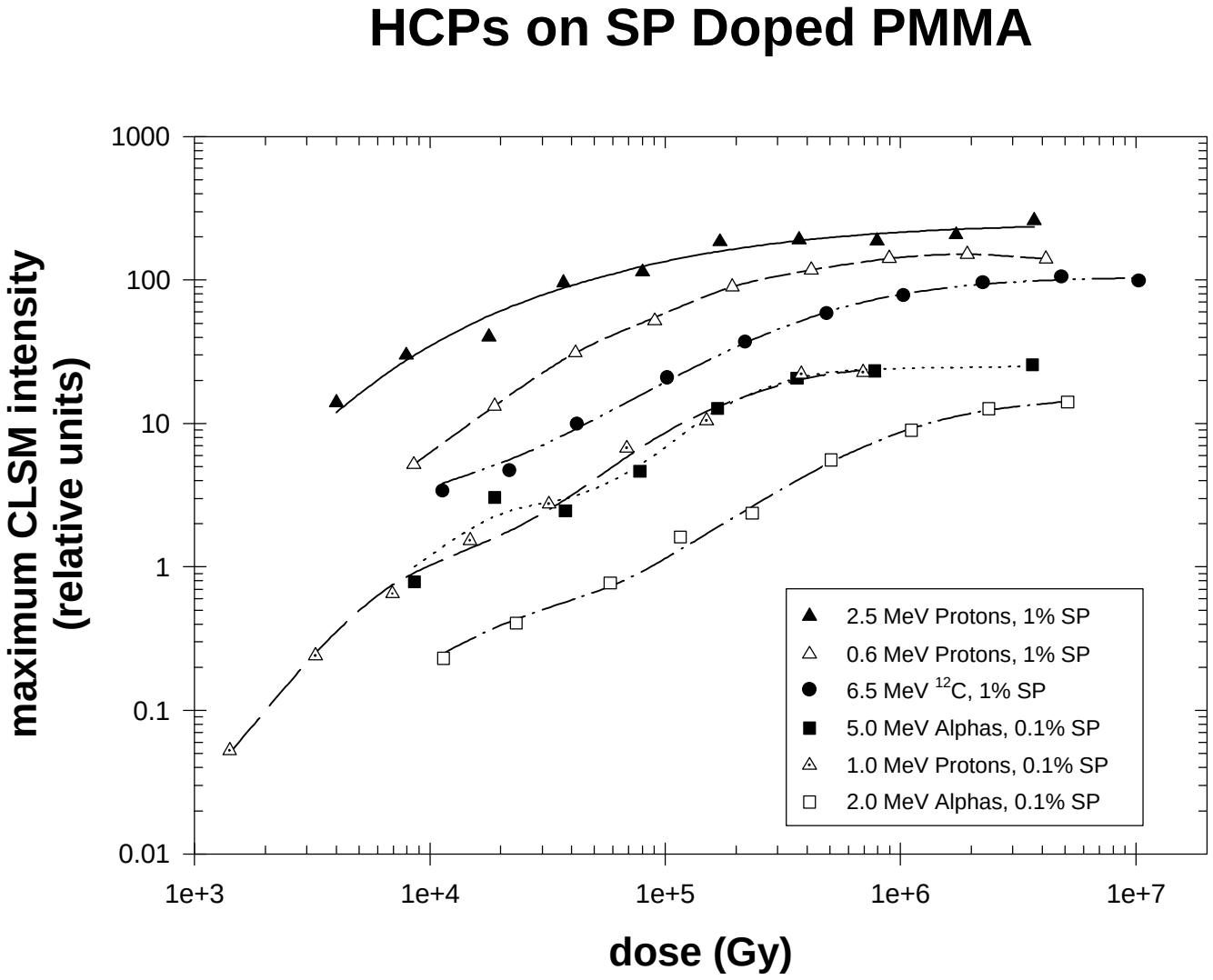

Figure 4. Maximum fluorescent intensities from the CLSM analysis plotted versus dose for the indicated particle and energy. The lines are smooth curves drawn through the data.

Device Characteristics

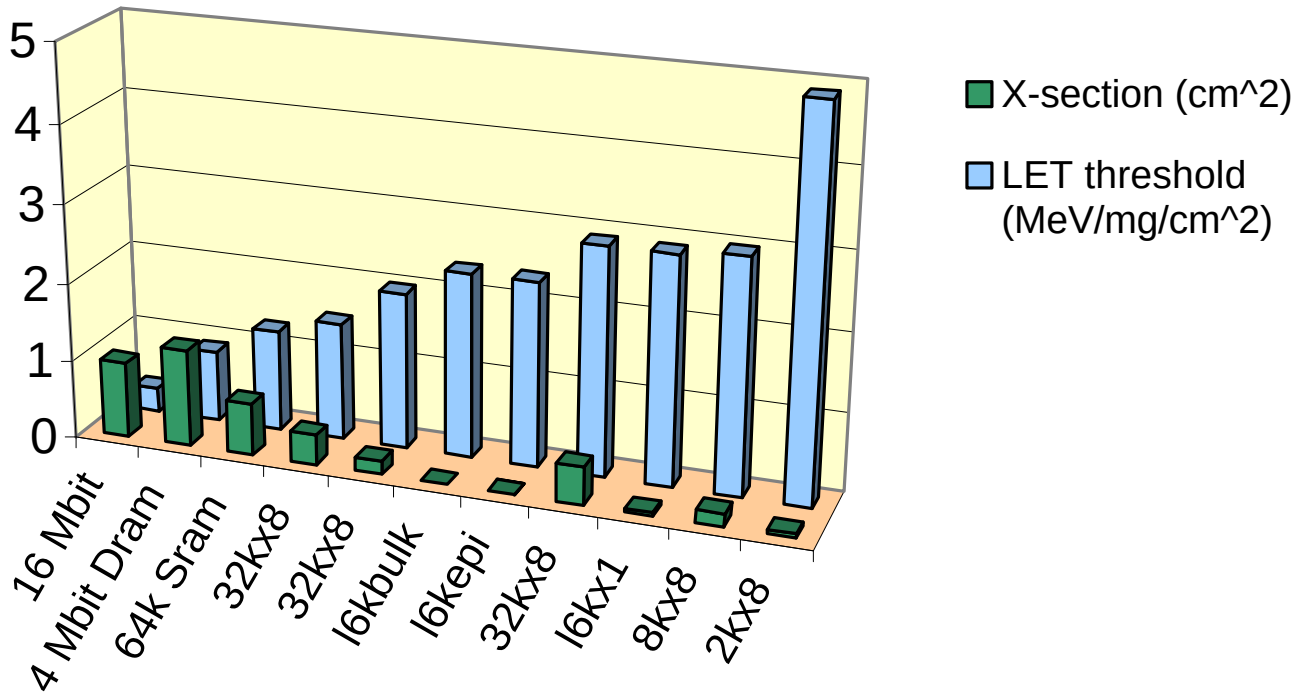

Figure 5. SEU cross-sections for representative computer memory devices (front) and LET thresholds (back). As the number of bits per chip increases from right to left (and feature size decreases) the LET threshold goes down and the SEU cross section goes up.